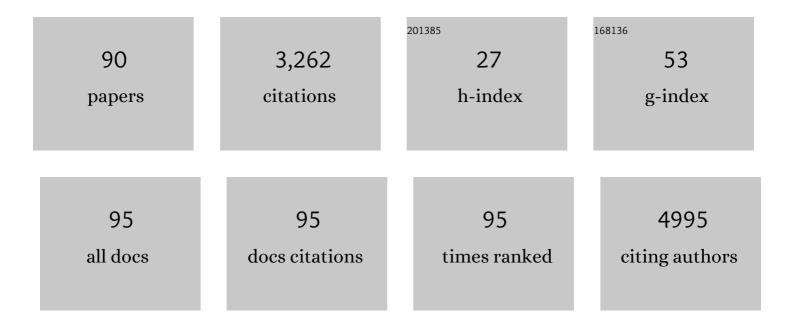
Chan-Gi Pack

List of Publications by Year in descending order

Source: https://exaly.com/author-pdf/5543688/publications.pdf Version: 2024-02-01



#	Article	IF	CITATIONS
1	The A- and B-type nuclear lamin networks: microdomains involved in chromatin organization and transcription. Genes and Development, 2008, 22, 3409-3421.	2.7	433
2	Cytosolic chaperonin prevents polyglutamine toxicity with altering the aggregation state. Nature Cell Biology, 2006, 8, 1163-1169.	4.6	252
3	Exosomal PD-L1 promotes tumor growth through immune escape in non-small cell lung cancer. Experimental and Molecular Medicine, 2019, 51, 1-13.	3.2	194
4	Local Nucleosome Dynamics Facilitate Chromatin Accessibility in Living Mammalian Cells. Cell Reports, 2012, 2, 1645-1656.	2.9	175
5	Interphase phosphorylation of lamin A. Journal of Cell Science, 2014, 127, 2683-96.	1.2	134
6	Advances in Analysis of Biodistribution of Exosomes by Molecular Imaging. International Journal of Molecular Sciences, 2020, 21, 665.	1.8	131
7	Microenvironment and Effect of Energy Depletion in the Nucleus Analyzed by Mobility of Multiple Oligomeric EGFPs. Biophysical Journal, 2006, 91, 3921-3936.	0.2	126
8	Quantitative live-cell imaging reveals spatio-temporal dynamics and cytoplasmic assembly of the 26S proteasome. Nature Communications, 2014, 5, 3396.	5.8	111
9	Deep Tumor Penetration of Drug-Loaded Nanoparticles by Click Reaction-Assisted Immune Cell Targeting Strategy. Journal of the American Chemical Society, 2019, 141, 13829-13840.	6.6	88
10	Reciprocal interaction with G-actin and tropomyosin is essential for aquaporin-2 trafficking. Journal of Cell Biology, 2008, 182, 587-601.	2.3	86
11	Estrogen-related receptor gamma functions as a tumor suppressor in gastric cancer. Nature Communications, 2018, 9, 1920.	5.8	85
12	The regulator of the F1 motor: inhibition of rotation of cyanobacterial F1-ATPase by the É> subunit. EMBO Journal, 2006, 25, 4596-4604.	3.5	74
13	In vivo evidence for the fibrillar structures of Sup35 prions in yeast cells. Journal of Cell Biology, 2010, 190, 223-231.	2.3	65
14	Protective role of endogenous plasmalogens against hepatic steatosis and steatohepatitis in mice. Hepatology, 2017, 66, 416-431.	3.6	61
15	Extracellular vesicle-derived DNA for performing EGFR genotyping of NSCLC patients. Molecular Cancer, 2018, 17, 15.	7.9	57
16	In vivo stepwise immunomodulation using chitosan nanoparticles as a platform nanotechnology for cancer immunotherapy. Scientific Reports, 2016, 6, 38348.	1.6	55
17	Proteome-wide discovery of mislocated proteins in cancer. Genome Research, 2013, 23, 1283-1294.	2.4	49
18	Dynamics of yeast prion aggregates in single living cells. Genes To Cells, 2006, 11, 1085-1096.	0.5	46

#	Article	IF	CITATIONS
19	Analysis of interaction between chaperonin GroEL and its substrate using fluorescence correlation spectroscopy. Cytometry, 1999, 36, 247-253.	1.8	45
20	Flexible and dynamic nucleosome fiber in living mammalian cells. Nucleus, 2013, 4, 349-356.	0.6	42
21	RNA-binding protein NONO contributes to cancer cell growth and confers drug resistance as a theranostic target in TNBC. Theranostics, 2020, 10, 7974-7992.	4.6	42
22	Mesenchymal stem cells prevent the progression of diabetic nephropathy by improving mitochondrial function in tubular epithelial cells. Experimental and Molecular Medicine, 2019, 51, 1-14.	3.2	39
23	Label-free high-resolution 3-D imaging of gold nanoparticles inside live cells using optical diffraction tomography. Methods, 2018, 136, 160-167.	1.9	38
24	Effect of Electrostatic Interactions on the Binding of Charged Substrate to GroEL Studied by Highly Sensitive Fluorescence Correlation Spectroscopy. Biochemical and Biophysical Research Communications, 2000, 267, 300-304.	1.0	36
25	A novel sphingomyelin/cholesterol domainâ€specific probe reveals the dynamics of the membrane domains during virus release and in Niemannâ€Pick type C. FASEB Journal, 2017, 31, 1301-1322.	0.2	34
26	Transient Acceleration of Epidermal Growth Factor Receptor Dynamics Produces Higher-Order Signaling Clusters. Journal of Molecular Biology, 2018, 430, 1386-1401.	2.0	34
27	Single mother–daughter pair analysis to clarify the diffusion properties of yeast prion Sup35 in guanidineâ€HClâ€treated [<i>PSI</i> ⁺] cells. Genes To Cells, 2009, 14, 1045-1054.	0.5	32
28	Fluorescence correlation spectroscopy analysis of the hydrophobic interactions of protein 4.1 with phosphatidyl serine liposomes. Biophysical Chemistry, 1999, 82, 149-155.	1.5	29
29	Exosomal miR-1260b derived from non-small cell lung cancer promotes tumor metastasis through the inhibition of HIPK2. Cell Death and Disease, 2021, 12, 747.	2.7	29
30	Dynamic and coordinated singleâ€molecular interactions at TM4SF5â€enriched microdomains guide invasive behaviors in 2―and 3â€dimensional environments. FASEB Journal, 2017, 31, 1461-1481.	0.2	26
31	Cortical Polarity of the RING Protein PAR-2 Is Maintained by Exchange Rate Kinetics at the Cortical-Cytoplasmic Boundary. Cell Reports, 2016, 16, 2156-2168.	2.9	25
32	Fecal microbiota transplantation ameliorates atherosclerosis in mice with C1q/TNF-related protein 9 genetic deficiency. Experimental and Molecular Medicine, 2022, 54, 103-114.	3.2	25
33	Light-Induced Fluorescence Modulation of Quantum Dot-Crystal Violet Conjugates: Stochastic Off–On–Off Cycles for Multicolor Patterning and Super-Resolution. Journal of the American Chemical Society, 2017, 139, 7603-7615.	6.6	24
34	Physicochemical Properties of Nucleoli in Live Cells Analyzed by Label-Free Optical Diffraction Tomography. Cells, 2019, 8, 699.	1.8	24
35	Assembly of protein complexes restricts diffusion of Wnt3a proteins. Communications Biology, 2018, 1, 165.	2.0	23
36	Live cell single-molecule detection in systems biology. Wiley Interdisciplinary Reviews: Systems Biology and Medicine, 2012, 4, 183-192.	6.6	21

#	Article	IF	CITATIONS
37	Heat shock instructs hESCs to exit from the self-renewal program through negative regulation of OCT4 by SAPK/JNK and HSF1 pathway. Stem Cell Research, 2013, 11, 1323-1334.	0.3	21
38	Photosystem II antenna phosphorylation-dependent protein diffusion determined by fluorescence correlation spectroscopy. Scientific Reports, 2013, 3, 2833.	1.6	20
39	Mitotic Chromosomes in Live Cells Characterized Using High-Speed and Label-Free Optical Diffraction Tomography. Cells, 2019, 8, 1368.	1.8	20
40	Interaction of a Small Heat Shock Protein of the Fission Yeast, Schizosaccharomyces pombe, with a Denatured Protein at Elevated Temperature. Journal of Biological Chemistry, 2005, 280, 32586-32593.	1.6	19
41	Dynamic and unique nucleolar microenvironment revealed by fluorescence correlation spectroscopy. FASEB Journal, 2015, 29, 837-848.	0.2	19
42	Single-particle tracking of quantum dot-conjugated prion proteins inside yeast cells. Biochemical and Biophysical Research Communications, 2011, 405, 638-643.	1.0	18
43	Characterization of the Triplet State of Hybridization-Sensitive DNA Probe by Using Fluorescence Correlation Spectroscopy. Journal of Physical Chemistry A, 2013, 117, 27-33.	1.1	18
44	Fabrication of a silver particle-integrated silicone polymer-covered metal stent against sludge and biofilm formation and stent-induced tissue inflammation. Scientific Reports, 2016, 6, 35446.	1.6	18
45	Optimization of ZnO Nanorod-Based Surface Enhanced Raman Scattering Substrates for Bio-Applications. Nanomaterials, 2019, 9, 447.	1.9	18
46	Apolipoprotein E-mediated regulation of selenoprotein P transportation via exosomes. Cellular and Molecular Life Sciences, 2020, 77, 2367-2386.	2.4	17
47	An aniline bearing hemicyanine derivative serves as a mitochondria selective probe. Dyes and Pigments, 2017, 136, 467-472.	2.0	16
48	[PSI+] aggregate enlargement in rnq1 nonprion domain mutants, leading to a loss of prion in yeast. Genes To Cells, 2011, 16, 576-589.	0.5	15
49	Microenvironments and different nanoparticle dynamics in living cells revealed by a standard nanoparticle. Journal of Controlled Release, 2012, 163, 315-321.	4.8	14
50	Quantitative analyses reveal extracellular dynamics of Wnt ligands in Xenopus embryos. ELife, 2021, 10,	2.8	14
51	Safety and efficacy of a metal stent covered with a silicone membrane containing integrated silver particles in preventing biofilm and sludge formation in endoscopic drainage of malignant biliary obstruction: a phase 2 pilot study. Gastrointestinal Endoscopy, 2019, 90, 663-672.e2.	0.5	13
52	ADAR1 Suppresses Interferon Signaling in Gastric Cancer Cells by MicroRNA-302a-Mediated IRF9/STAT1 Regulation. International Journal of Molecular Sciences, 2020, 21, 6195.	1.8	13
53	miR-351-5p/Miro2 axis contributes to hippocampal neural progenitor cell death via unbalanced mitochondrial fission. Molecular Therapy - Nucleic Acids, 2021, 23, 643-656.	2.3	13
54	Combinatory RNA-Sequencing Analyses Reveal a Dual Mode of Gene Regulation by ADAR1 in Gastric Cancer. Digestive Diseases and Sciences, 2018, 63, 1835-1850.	1.1	12

#	Article	IF	CITATIONS
55	Global analysis of protein homomerization in <i>Saccharomyces cerevisiae</i> . Genome Research, 2019, 29, 135-145.	2.4	12
56	Characterizing Organelles in Live Stem Cells Using Label-Free Optical Diffraction Tomography. Molecules and Cells, 2021, 44, 851-860.	1.0	10
57	Diffusion analysis of glucocorticoid receptor and antagonist effect in living cell nucleus. Experimental and Molecular Pathology, 2007, 82, 163-168.	0.9	9
58	Analysis of Quantum Rod Diffusion by Polarized Fluorescence Correlation Spectroscopy. Journal of Fluorescence, 2014, 24, 1371-1378.	1.3	8
59	Analyses of the Dynamic Properties of Nuclear Lamins by Fluorescence Recovery After Photobleaching (FRAP) and Fluorescence Correlation Spectroscopy (FCS). Methods in Molecular Biology, 2016, 1411, 99-111.	0.4	8
60	Detection of substrate binding of a collagen-specific molecular chaperone HSP47 in solution using fluorescence correlation spectroscopy. Biochemical and Biophysical Research Communications, 2018, 497, 279-284.	1.0	8
61	A bipolar functionality of Q/Nâ€rich proteins: Lsm4 amyloid causes clearance of yeast prions. MicrobiologyOpen, 2013, 2, 415-430.	1.2	7
62	Heat shock-induced interactions among nuclear HSFs detected by fluorescence cross-correlation spectroscopy. Biochemical and Biophysical Research Communications, 2015, 463, 303-308.	1.0	7
63	Diagnosis in a Preclinical Model of Bladder Pain Syndrome Using a Au/ZnO Nanorod-based SERS Substrate. Nanomaterials, 2019, 9, 224.	1.9	7
64	Heterogeneous interaction network of yeast prions and remodeling factors detected in live cells. BMB Reports, 2017, 50, 478-483.	1,1	7
65	Label-free imaging and evaluation of characteristic properties of asthma-derived eosinophils using optical diffraction tomography. Biochemical and Biophysical Research Communications, 2022, 587, 42-48.	1.0	7
66	Radiationless deactivation of hybridization-sensitive DNA probe. Journal of Luminescence, 2012, 132, 2566-2571.	1.5	6
67	The interaction of Hsp104 with yeast prion Sup35 as analyzed by fluorescence cross-correlation spectroscopy. Biochemical and Biophysical Research Communications, 2013, 442, 28-32.	1.0	6
68	Novel Compound Heterozygote Mutation in <i>IL10RA</i> in a Patient With Very Early-Onset Inflammatory Bowel Disease. Inflammatory Bowel Diseases, 2019, 25, 498-509.	0.9	6
69	Yeast beta-glucan mediates histone deacetylase 5-induced angiogenesis in vascular endothelial cells. International Journal of Biological Macromolecules, 2022, 211, 556-567.	3.6	6
70	Integrative microendoscopic system combined with conventional microscope for live animal tissue imaging. Journal of Biophotonics, 2018, 11, e201800206.	1,1	5
71	Variably Sized and Multi-Colored Silica-Nanoparticles Characterized by Fluorescence Correlation Methods for Cellular Dynamics. Materials, 2021, 14, 19.	1.3	5
72	Diffusion Coefficients of CdSe/CdS Quantum Rods in Water Measured Using Polarized Fluorescence Correlation Spectroscopy. Journal of the Optical Society of Korea, 2014, 18, 598-604.	0.6	5

#	Article	IF	CITATIONS
73	SERS Effect on Spin-Coated Seeding of Tilted Au-ZnO Nanorods for Low-Cost Diagnosis. Materials, 2020, 13, 5321.	1.3	4
74	Confocal Laser Scanning Microscopy and Fluorescence Correlation Methods for the Evaluation of Molecular Interactions. Advances in Experimental Medicine and Biology, 2021, 1310, 1-30.	0.8	4
75	Interpretation of <i>XIAP</i> Variants of Uncertain Significance in Paediatric Patients with Refractory Crohn's Disease. Journal of Crohn's and Colitis, 2021, 15, 1291-1304.	0.6	4
76	FTIR study of the surface-ligand exchange reaction with glutathione on biocompatible rod-shaped CdSe/CdS semiconductor nanocrystals. Physical Chemistry Chemical Physics, 2022, 24, 13356-13364.	1.3	4
77	Application of quantitative cell imaging using label-free optical diffraction tomography. Biophysics and Physicobiology, 2021, 18, 244-253.	0.5	3
78	Smart Vitamin Micelles as Cancer Nanomedicines for Enhanced Intracellular Delivery of Doxorubicin. International Journal of Molecular Sciences, 2021, 22, 11298.	1.8	3
79	Use of Engineered Nanoparticle-Based Fluorescence Methods for Live-Cell Phenomena. , 2014, , 153-169.		2
80	Large-scale analysis of diffusional dynamics of proteins in living yeast cells using fluorescence correlation spectroscopy. Biochemical and Biophysical Research Communications, 2019, 520, 237-242.	1.0	2
81	SLAC2Bâ€dependent microtubule acetylation regulates extracellular matrixâ€mediated intracellular TM4SF5 traffic to the plasma membranes. FASEB Journal, 2021, 35, e21369.	0.2	2
82	Phosphorescence decay time measurements using intensity correlation spectroscopy. Experimental and Molecular Pathology, 2007, 82, 175-183.	0.9	1
83	Clearance of yeast eRF-3 prion [<i>PSI</i> +] by amyloid enlargement due to the imbalance between chaperone Ssa1 and cochaperone Sgt2. Translation, 2013, 1, e26574.	2.9	1
84	Correlative Light and Electron Microscopy for Nanoparticle–Cell Interaction and Protein Localization. Advances in Experimental Medicine and Biology, 2021, 1310, 115-132.	0.8	1
85	Immuno-gold Techniques in Biomedical Sciences. Advances in Experimental Medicine and Biology, 2021, 1310, 133-152.	0.8	1
86	1P346 Oxygen concentration measurements by a phosphorescence intensity correlation method(New) Tj ETQc	0 0 0 rgBT	Overlock 10
87	Peptide sequences converting polyglutamine into a prion in yeast. FEBS Journal, 2015, 282, 477-490.	2.2	0
88	Poly(A)+ Sensing of Hybridization-Sensitive Fluorescent Oligonucleotide Probe Characterized by Fluorescence Correlation Methods. International Journal of Molecular Sciences, 2021, 22, 6433.	1.8	0
89	Mobility of Nucleostemin in Live Cells Is Specifically Related to Transcription Inhibition by Actinomycin D and GTP-Binding Motif. International Journal of Molecular Sciences, 2021, 22, 8293.	1.8	0

⁹⁰Application of Quantitative Cell Imaging Using Label-free Optical Diffraction Tomography. Seibutsu
Butsuri, 2020, 60, 352-355.0.00